It has been unclear whether the TCR generates similar signals for the development of effector and memory T cells. Our results and others' (*3*–*5*) suggest that effector and memory differentiation require a different set of signals. Our data are consistent with a two-lineage model where memory or effector development is determined very early during the immune response by coordinating the recruitment of fate-determining proteins at the level of the IS.

Our studies suggest that different T cell programs are triggered by qualitatively distinct TCR signals, which implies that unique signaling pathways are important for T cell memory development. Several molecules, such as B cell lymphoma–6 (Bcl-6), the B and T lymphocyte attenuator (BTLA), and methyl-CpG binding domain protein 2 (MBD2), are selectively important for memory development but not for effector differentiation (*21*–*23*). Along the same lines, mutant T cells are uniquely defective in memory development and NF-κB signaling. Several studies have reported a role for members of the NF-κB signaling pathway in memory development (*24*, *25*).

Our studies emphasize the importance of the TCR in regulating the NF-κB signal required for memory development. We show here that effector and memory programming can be dissociated by the induction of a different arrangement of TCR signals in $CD8^+$ T cells. Studying how these TCR signals are modulated by inflammatory signals or $CD4^+$ help will be important in the design of better vaccination regimes.

References and Notes

1. S. M. Kaech, S. Hemby, E. Kersh, R. Ahmed, *Cell* **111**, 837 (2002).
2. J. T. Opferman, B. T. Ober, P. G. Ashton-Rickardt, *Science* **283**, 1745 (1999).
3. G. Lauvau *et al.*, *Science* **294**, 1735 (2001).
4. V. P. Badovinac, K. A. Messingham, A. Jabbari, J. S. Haring, J. T. Harty, *Nat. Med.* **11**, 748 (2005).
5. J. T. Chang *et al.*, *Science* **315**, 1687 (2007).
6. N. S. Joshi *et al.*, *Immunity* **27**, 281 (2007).
7. J. T. Harty, V. P. Badovinac, *Nat. Rev. Immunol.* **8**, 107 (2008).
8. A. Lanzavecchia, F. Sallusto, *Nat. Rev. Immunol.* **2**, 982 (2002).
9. M. J. van Stipdonk *et al.*, *Nat. Immunol.* **4**, 361 (2003).
10. M. Prlic, G. Hernandez-Hoyos, M. J. Bevan, *J. Exp. Med.* **203**, 2135 (2006).
11. M. A. Williams, E. V. Ravkov, M. J. Bevan, *Immunity* **28**, 533 (2008).
12. T. R. Mempel, S. E. Henrickson, U. H. Von Andrian, *Nature* **427**, 154 (2004).
13. K. S. Campbell, B. T. Backstrom, G. Tiefenthaler, E. Palmer, *Semin. Immunol.* **6**, 393 (1994).
14. E. Teixeiro *et al.*, *Immunity* **21**, 515 (2004).
15. E. Teixeiro, A. Garcia-Sahuquillo, B. Alarcon, R. Bragado, *Eur. J. Immunol.* **29**, 745 (1999).
16. Materials and methods are available as supporting material on *Science* Online.
17. Single-letter abbreviations for the amino acid residues are as follows: A, Ala; C, Cys; D, Asp; E, Glu; F, Phe; G, Gly; H, His; I, Ile; K, Lys; L, Leu; M, Met; N, Asn; P, Pro; Q, Gln; R, Arg; S, Ser; T, Thr; V, Val; W, Trp; and Y, Tyr.
18. K. A. Hogquist *et al.*, *Cell* **76**, 17 (1994).
19. J. Hataye, J. J. Moon, A. Khoruts, C. Reilly, M. K. Jenkins, *Science* **312**, 114 (2006).
20. M. A. Williams, M. J. Bevan, *Annu. Rev. Immunol.* **25**, 171 (2007).
21. H. Ichii *et al.*, *Nat. Immunol.* **3**, 558 (2002).
22. C. Krieg, O. Boyman, Y. X. Fu, J. Kaye, *Nat. Immunol.* **8**, 162 (2007).
23. E. N. Kersh, *J. Immunol.* **177**, 3821 (2006).
24. T. Hettmann, J. T. Opferman, J. M. Leiden, P. G. Ashton-Rickardt, *Immunol. Lett.* **85**, 297 (2003).
25. M. Schmidt-Supprian *et al.*, *Immunity* **19**, 377 (2003).

26. We thank D. Roubaty, B. Hausmann, V. Jäggin, G. E. Fernandez, H. Karauzum, M. Schmaler, and Z. Rajacic for technical assistance; R. Landmann-Suter for technical advice; and C. Pernas Pernas for helpful discussion. This work was supported by Mission Enhancement Program, University of Missouri (E.T. and M.A.D.) fellowships from the Fundación Ramón Areces, Spain (E.T.), the American Cancer Society (S.E.H.), the Cancer Research Institute (M.A.D.), the Spanish Ministry of Science and Education (MEC) (BFU 2005-02807) (R.B.), Novartis, Roche, Sybilla (EUFP7) and the Swiss National Science Foundation (E.P.).

Supporting Online Material
www.sciencemag.org/cgi/content/full/323/5913/502/DC1
Materials and Methods
Figs. S1 to S7
References
Movies S1 to S4

22 July 2008; accepted 26 November 2008
10.1126/science.1163612

Secondary Replicative Function of $CD8^+$ T Cells That Had Developed an Effector Phenotype

Oliver Bannard, Matthew Kraman, Douglas T. Fearon*

Models of the differentiation of memory $CD8^+$ T cells that replicate during secondary infections differ over whether such cells had acquired effector function during primary infections. We created a transgenic mouse line that permits mapping of the fate of granzyme B (gzmB)–expressing $CD8^+$ T cells and their progeny by indelibly marking them with enhanced yellow fluorescent protein (EYFP). Virus-specific $CD8^+$ T cells express gzmB within the first 2 days of a primary response to infection with influenza, without impairment of continued primary clonal expansion. On secondary infection, virus-specific $CD8^+$ T cells that became $EYFP^+$ during a primary infection clonally expand as well as all virus-specific $CD8^+$ T cells. Thus, $CD8^+$ T cells that have acquired an effector phenotype during primary infection may function as memory cells with replicative function.

During a primary immune response, naïve, pathogen-specific $CD8^+$ T cells replicate and generate effector cells that control the primary infection, and "memory" cells that persist after resolution of the primary infection and respond to secondary infections. Two types of memory cells have been identified: a subset that resides in the peripheral tissues and has immediate effector function, such as production of interferon-γ (IFN-γ) and cytolytic activity, but cannot replicate, and a subset that maintains a capacity for clonal expansion and generation of effector cells that are required for control of secondary or persistent infections (*1*). Because a single, antigen-specific $CD8^+$ T cell can give rise to primary effector cells and both types of memory cells (*2*), only two models are possible for the development of memory cells with replicative potential: They arise directly from naïve $CD8^+$ T cells and avoid effector differentiation (*3*), perhaps by a process of asymmetrical division (*4*), or they come from proliferating cells that have acquired effector function but have not irreversibly lost replicative capability (*5*, *6*). Determining which model is correct is necessary to guide experimental approaches to defining optimal vaccine strategies. We generated a mouse model that enables conditional, irreversible marking of $CD8^+$ T cells that have acquired an effector function, the expression of the cytolytic granule protein, granzyme B (gzmB). In the asymmetrical division model, gzmB expression is considered to identify the daughter T cell that is committed to loss of secondary replicative function (*4*).

We created a transgenic mouse line using a bacterial artificial chromosome (BAC) containing the *gzmB* gene, which had been modified by inserting at the start codon the tamoxifen-inducible, site-specific recombinase, $CreER^{T2}$ (fig. S1) (*7*, *8*). We crossed this $gzmBCreER^{T2}$ BAC transgenic line with the ROSA26EYFP reporter line in which enhanced yellow fluorescent protein (EYFP) is expressed following CreERT2-mediated excision of a loxP-flanked stop codon (*9*). Thus, in $gzmBER^{T2}$/ROSAEYFP mice, cells that transcribe the *gzmB* gene will express $CreER^{T2}$, but such cells may become $EYFP^+$ only in the presence of tamoxifen. This enables the fate-mapping of such cells without the need for adoptive transfer, which may alter the dynamics of clonal expansion (*10*). Furthermore, a BAC transgene containing the *gzmB* gene for regulating expression of the

Wellcome Trust Immunology Unit, Department of Medicine, University of Cambridge, Medical Research Council Centre, Hills Road, Cambridge CB2 2QH, UK.

*To whom correspondence should be addressed. E-mail: dtf1000@cam.ac.uk

Cre recombinase circumvents the problem of earlier studies (*11*) using a truncated human *GzmB* promoter that did not accurately reflect expression of the endogenous *gzmB* gene (*12*).

A requirement for both *gzmB* transcription and tamoxifen to induce EYFP was assessed by culturing $CD8^+$ T cells from gzmBCreER^{T2}/ROSA26EYFP mice in gzmB-inducing or noninducing conditions, with or without 4-hydroxytamoxifen (4-OHT). EYFP was observed only with culture conditions that induced gzmB synthesis by $CD8^+$ T cells in the presence of 4-OHT (Fig. 1A). $CD8^+$ T cells from the lungs of mice on day 10 of influenza infection were $EYFP^+$ also only if tamoxifen had been present (Fig. 1B). EYFP was expressed only by antigen-experienced, $CD44^{high}$ $CD4^+$ and $CD8^+$ T cells at day 10 and day 100 post infection (p.i.) (Fig. 1C), and by NK cells, but not by B cells, dendritic cells, or myelomonocytic cells (Fig. 1D). Therefore, induction of EYFP is stringently restricted to cells expressing gzmB in the presence of tamoxifen. The proportion of $EYFP^+$ cells correlated with the magnitude of gzmB expression (fig. S2), which suggested that inefficient Cre-mediated recombination accounted for the occurrence of gzmB-expressing $CD8^+$ T cells that were $EYFP^-$, despite the presence of tamoxifen.

To determine whether gzmB expression by $CD8^+$ T cells early during a primary response impairs clonal expansion, mice were infected intranasally with influenza, pulsed with tamoxifen on days 1 and 2 or days 7 and 8 p.i., and assessed on day 10 p.i. for the presence in the lungs and mediastinal lymph nodes (MLNs) of $EYFP^+$ $CD8^+$ T cells that were specific for the H–$2D^b$/nucleoprotein (NP) peptide complex. D^b/NP-specific $CD8^+$ T cells in the MLNs were $EYFP^+$ even when tamoxifen was given only during the initial phase of clonal expansion, which indicated that gzmB is expressed by virus-specific $CD8^+$ T cells in the first few cell cycles (*13*) and that such cells continue to proliferate and generate $EYFP^+$ cells that migrate to the lungs (Fig. 2A). Their continued replication was confirmed by incorporation of 5-bromo-2′-deoxyuridine (BrdU) during days 5 to 9 (Fig. 2B). Administering tamoxifen on days 7 and 8 induced only slightly higher percentages of $EYFP^+$ cells among the D^b/NP-specific populations, corroborating that early gzmB expression does not impair subsequent clonal expansion. Finally, the pulse characteristics of tamoxifen-mediated CreER^{T2} function were confirmed by the absence of $EYFP^+$ D^b/NP-specific $CD8^+$ T cells in mice that had received tamoxifen on the 2 days preceding viral infection (Fig. 2A).

The capacity to mark irreversibly a cohort of cells that had expressed gzmB permitted an analysis of changes in their phenotypic characteristics over time. On day 10 of the primary response to influenza with tamoxifen administered on days 1 to 8, almost all $EYFP^+$ $CD8^+$ T cells in the lungs and spleen expressed gzmB, whereas a subset of $EYFP^+$ cells in the MLNs had become $gzmB^-$ (Fig. 3A). By day 49, most $EYFP^+$ $CD8^+$ T cells had lost expression of gzmB except for a small subpopulation in the lungs. A decrease in gzmB expression among virus-specific $CD8^+$ T cells during the phase following clearance of a primary infection has been considered to exemplify a requirement for a "rest" period during which effector cells convert to memory cells (*5*). The present finding that $CD8^+$ T cells have the capacity to switch gzmB expression on and off during the acute phase of the primary response suggests that decreased biosynthesis may be caused by diminished inducing signals, at least within the MLN. Consistent with this possibility, when tamoxifen was administered on days 1 to 4 p.i. and BrdU during the last 12 hours, before analysis on day 8 p.i., the $EYFP^+$ $CD8^+$

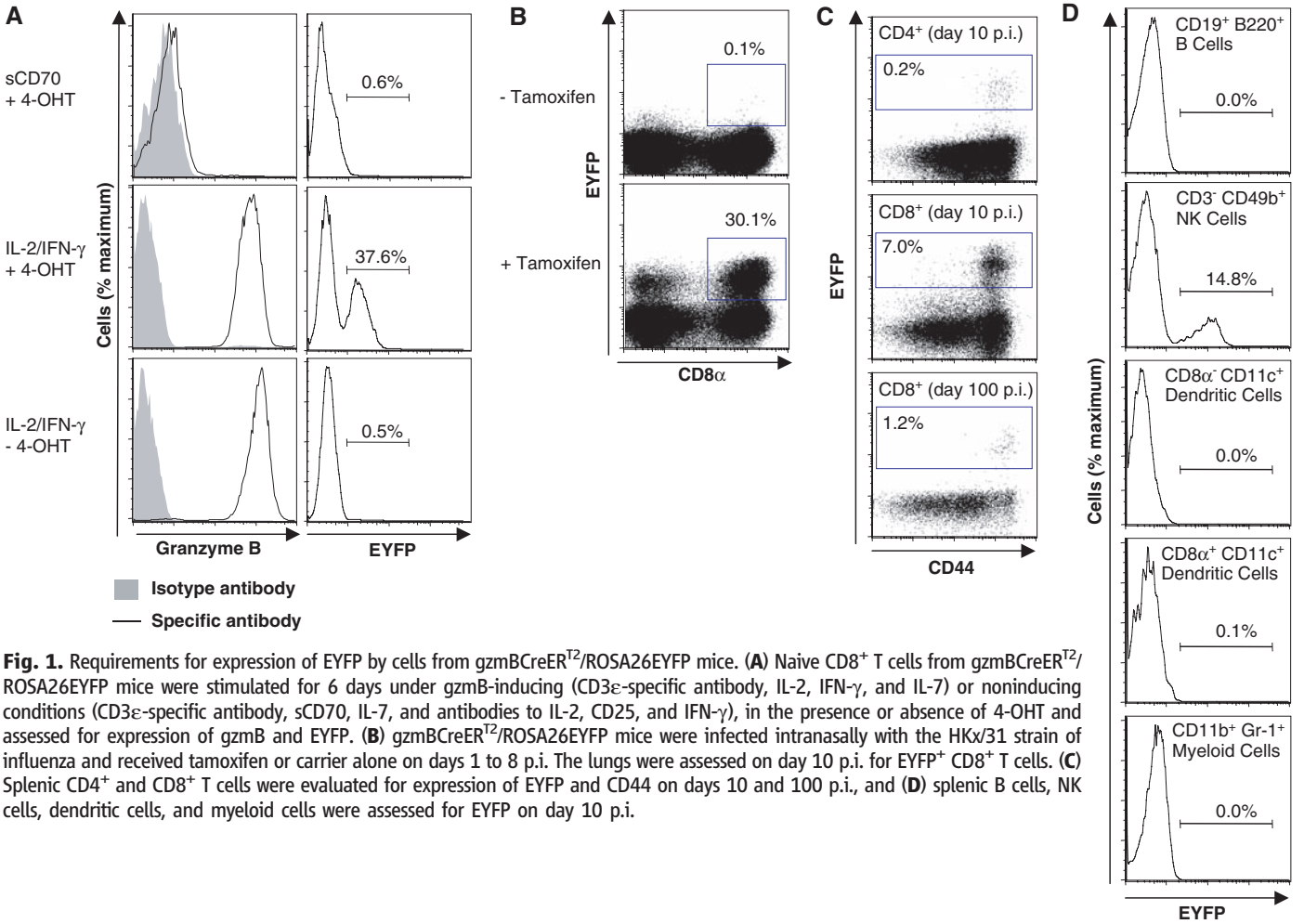

Fig. 1. Requirements for expression of EYFP by cells from gzmBCreER^{T2}/ROSA26EYFP mice. (**A**) Naive $CD8^+$ T cells from gzmBCreER^{T2}/ROSA26EYFP mice were stimulated for 6 days under gzmB-inducing (CD3ε-specific antibody, IL-2, IFN-γ, and IL-7) or noninducing conditions (CD3ε-specific antibody, sCD70, IL-7, and antibodies to IL-2, CD25, and IFN-γ), in the presence or absence of 4-OHT and assessed for expression of gzmB and EYFP. (**B**) gzmBCreER^{T2}/ROSA26EYFP mice were infected intranasally with the HKx/31 strain of influenza and received tamoxifen or carrier alone on days 1 to 8 p.i. The lungs were assessed on day 10 p.i. for $EYFP^+$ $CD8^+$ T cells. (**C**) Splenic $CD4^+$ and $CD8^+$ T cells were evaluated for expression of EYFP and CD44 on days 10 and 100 p.i., and (**D**) splenic B cells, NK cells, dendritic cells, and myeloid cells were assessed for EYFP on day 10 p.i.

T cells lacking expression of gzmB were mainly $CD25^-$ and $BrdU^-$, whereas the $gzmB^+$ cells expressed high levels of CD25 and were $BrdU^+$ (Fig. 3B). Thus, loss of gzmB expression may reflect interrupted signaling through the interleukin 2 (IL-2) receptor.

The loss of expression of CD62L and IL-7Rα by $CD8^+$ T cells during the primary response correlates with diminished survival and replicative capability in the memory phase of the response (*5*, *6*). On day 10, $EYFP^+$ $CD8^+$ T cells in the MLNs, the site of clonal expansion, but not in the spleen or lungs, remained $CD62L^{high}$ (Fig. 3A). Therefore, diminished expression of CD62L is not necessarily linked to expression of gzmB, as has been suggested (*4*). By day 49, $CD62L^{high}$ $EYFP^+$ $CD8^+$ T cells were also present in the spleen, but not in the lung, which indicated either that, during the memory phase, $CD62L^{high}$ cells from the MLNs migrate to the lymphoid areas of the spleen; that there is selective loss of $CD62L^{low}$ cells in the spleen; or that both occur. Similarly, by day 42, $EYFP^+$ $CD8^+$ T cells expressing IL-7Rα were present in the MLNs and spleen, but all $EYFP^+$ cells in the lungs lacked this receptor (Fig. 3A). Therefore, the phenotype of $CD62L^{high}$ and IL-$7R\alpha^+$ of memory cells that have expressed gzmB correlates with their anatomic site and not with whether they have exhibited this differentiated function.

We examined whether $EYFP^+$ D^b/NP-specific $CD8^+$ T cells persisted into the memory phase and responded secondarily to influenza infection. The proportion of D^b/NP-specific $CD8^+$ T cells in the lungs, MLNs, and spleen that were $EYFP^+$ did not change between days 10 and

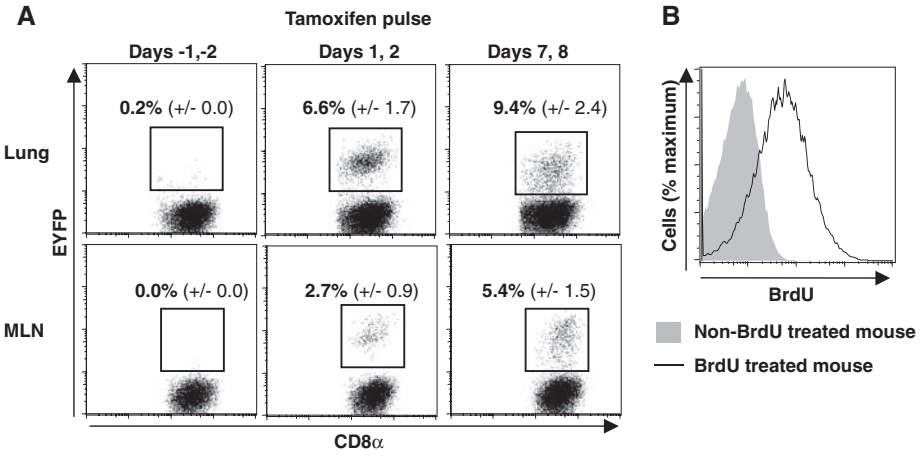

Fig. 2. Clonal expansion by $CD8^+$ T cells that had expressed gzmB during the first days of influenza infection. (**A**) gzmBCreER^{T2}/ROSA26EYFP mice were infected intranasally with the HKx/31 strain of influenza and were given tamoxifen for 2 days before infection, on days 1 and 2 p.i., or on days 7 and 8 p.i. On day 10 p.i., we determined the proportion (mean ± SEM) of D^b/NP-pentamer–binding $CD8^+$ T cells that was $EYFP^+$. (**B**) Influenza-infected mice that had received tamoxifen on days 1 and 2 were given BrdU on days 5 to 9 p.i., and $EYFP^+$ $CD8^+$ T cells from the lungs were assessed on day 10 p.i. for incorporation of BrdU.

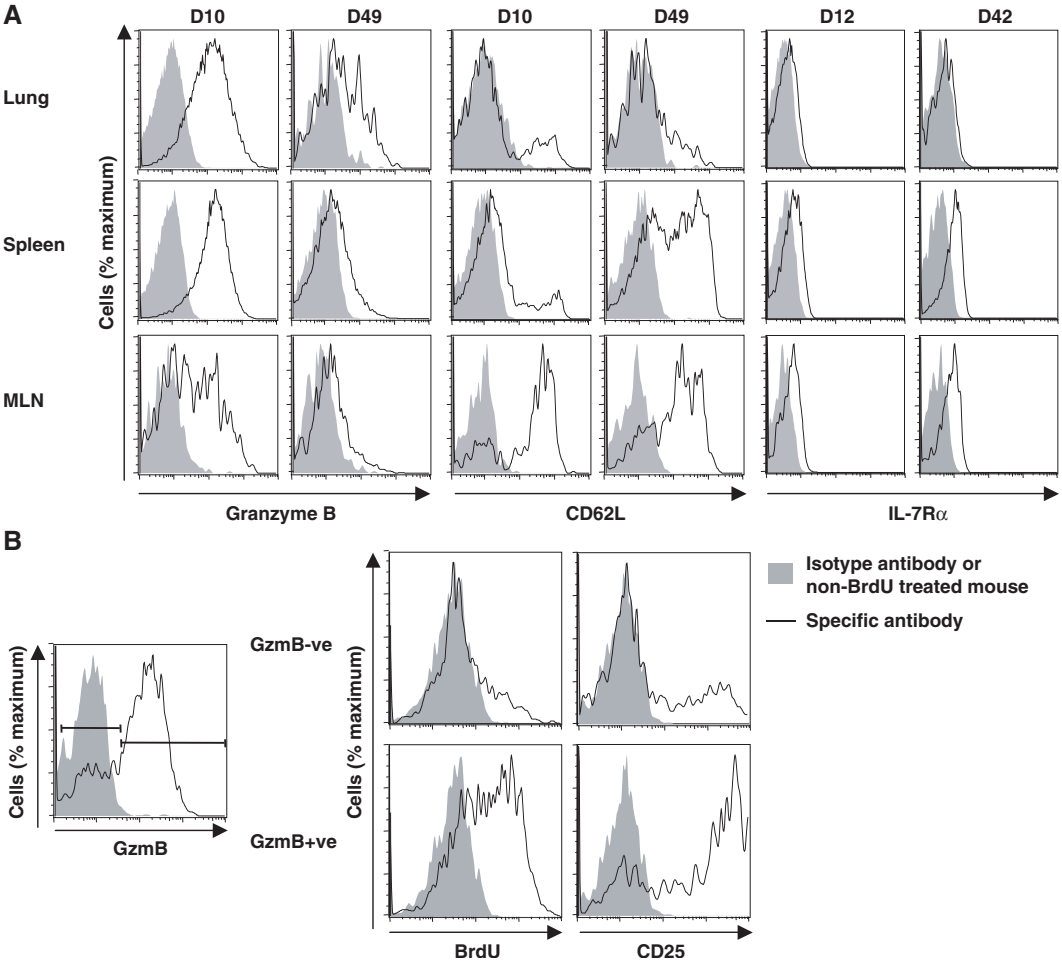

Fig. 3. Expression of gzmB, CD62L, IL-7Rα, and CD25 by $EYFP^+$ $CD8^+$ T cells responding to influenza infection. (**A**) gzmBCreER^{T2}/ROSA26EYFP mice were infected intranasally with the HKx/31 strain of influenza and treated with tamoxifen on days 1 to 8 p.i. The $EYFP^+$ $CD8^+$ T cells from the lungs, MLNs, and spleen were analyzed for intracellular gzmB, CD62L, and IL-7Rα at the peak of the primary response and during the memory phase (6 or 7 weeks p.i.). (**B**) Influenza-infected mice were given tamoxifen on days 1 to 4 p.i. and BrdU 12 hours before analysis on day 8 for BrdU incorporation and CD25 expression by $EYFP^+$ $CD8^+$ T cells from the MLNs.

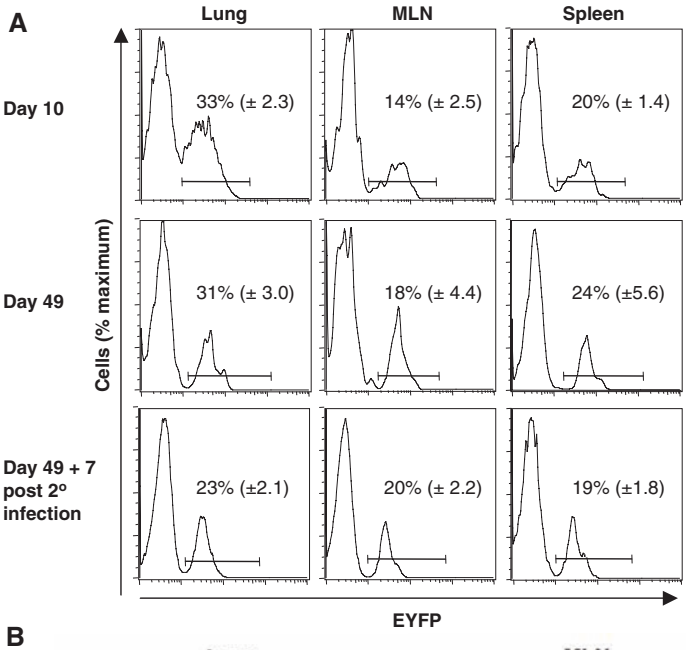

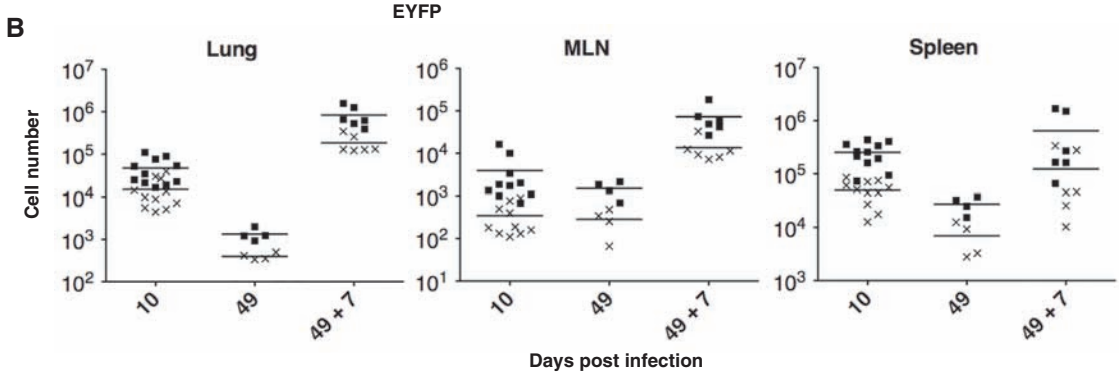

Fig. 4. Absence of impaired secondary clonal expansion by CD8$^+$ T cells that had expressed gzmB during primary influenza infection. gzmBCreER^{T2}/ROSA26EYFP mice were intranasally infected with the HKx/31 strain of influenza and given tamoxifen on days 1 to 8 p.i. On days 10 and 49 p.i., CD8$^+$ T cells from the lungs, MLNs, and spleens were assessed for the binding of D^b/NP pentamers and expression of EYFP$^+$. The mice were challenged on day 49 p.i. with the PR8 strain of influenza in the absence of tamoxifen, and the same measurements were performed 7 days later. (**A**) The proportions (mean ± SEM) of D^b/NP-specific CD8$^+$ T cells that were EYFP$^+$ are shown. (**B**) The numbers of total (squares) and EYFP$^+$ (crosses) D^b/NP-specific CD8$^+$ T cells in the lungs, MLNs, and spleens of each mouse are shown.

49 p.i. ($P > 0.4$), which indicated that expression of gzmB during the primary response does not destine a cell for contraction (Fig. 4A). Furthermore, the proportion of EYFP$^+$ D^b/NP-specific cells in the MLNs remained the same after secondary viral infection, which suggested that these cells replicated as well as all D^b/NP-specific memory CD8$^+$ T cells. The modest decrease in the percentage of EYFP$^+$ cells in the lungs after secondary expansion may reflect the presence at day 49 of cells that had been labeled at this peripheral site during the primary infection and were unable to replicate during the secondary infection.

Equivalent replicative capability of the EYFP$^+$ and total D^b/NP-specific CD8$^+$ T cells was confirmed by finding ~500-fold expansion of both populations in the lungs on day 7 post secondary infection (Fig. 4B). There were lower, although again comparable, increases in these two populations in the MLNs (Fig. 4B), where most new effector cells in the lungs are likely to be generated, and also in the spleen.

The capacity to replicate secondarily was also determined for EYFP$^+$ D^b/NP-specific CD8$^+$ T cells that had been marked by tamoxifen pulses on days 1 to 3 and days 7 to 9, respectively, during primary influenza infection. On day 7 post secondary infection, the EYFP$^+$ D^b/NP-specific CD8$^+$ T cells in the two groups had similar fold increments in the MLNs, spleens, and lungs, and these were comparable to those of the total antigen-specific cells (fig. S3). This finding further excludes models of differentiation in which early expression of gzmB marks a CD8$^+$ T cell that has lost a capacity for secondary replicative function.

In summary, the conditional and indelible marking of CD8$^+$ T cells that had previously expressed gzmB permitted their identification among all subsets of CD8$^+$ T cells in the primary and memory phases of an antiviral response, including the subset that mediates secondary clonal expansion. Combined with the observation that a CD8$^+$ T cell may express gzmB early in the primary response without preventing continued expansion (Fig. 2A), one may conclude that such cells can self-renew and serve as progenitors of the more differentiated, senescent cells that have diminished expression of CD62L and IL-7Rα (Fig. 3A). Although EYFP was not induced in all gzmB-expressing cells because of inefficient Cre-mediated recombination, the EYFP$^+$ memory CD8$^+$ T cell population was representative of the entire memory population with respect to survival and secondary expansion. Therefore, memory CD8$^+$ T cells that proliferate during secondary infections can be derived from cells that had acquired an effector phenotype during the primary response, as has been proposed (*5*, *6*). This conclusion is consistent with the IL-2R-dependence of gzmB expression (Fig. 3B) and development of memory cells with replicative function (*14*) and with the secondary replication of IFN-γ–expressing memory CD4$^+$ T cells (*15*). However, it does not support the asymmetrical division model in which the gzmB-expressing daughter cell of the first division of the activated naïve CD8$^+$ T cell is restricted to a nonreplicative memory cell fate (*4*). Thus, as-yet-undefined signals, in addition to those leading to acquisition of gzmB-dependent effector functions and that cannot be defined in this experimental system, must account for terminal differentiation and senescence of the CD8$^+$ T cell.

References and Notes

1. F. Sallusto, D. Lenig, R. Forster, M. Lipp, A. Lanzavecchia, *Nature* **401**, 708 (1999).
2. C. Stemberger *et al.*, *Immunity* **27**, 985 (2007).
3. D. T. Fearon, P. Manders, S. D. Wagner, *Science* **293**, 248 (2001).
4. J. T. Chang *et al.*, *Science* **315**, 1687 (2007).
5. E. J. Wherry *et al.*, *Nat. Immunol.* **4**, 225 (2003).
6. N. S. Joshi *et al.*, *Immunity* **27**, 281 (2007).
7. R. Feil, J. Wagner, D. Metzger, P. Chambon, *Biochem. Biophys. Res. Commun.* **237**, 752 (1997).

8. Materials and methods are available as supporting material on *Science* Online.
9. S. Srinivas *et al.*, *BMC Dev. Biol.* **1**, 4 (2001).
10. A. L. Marzo *et al.*, *Nat. Immunol.* **6**, 793 (2005).
11. J. Jacob, D. Baltimore, *Nature* **399**, 593 (1999).
12. R. D. Hanson, G. M. Sclar, O. Kanagawa, T. J. Ley, *J. Biol. Chem.* **266**, 24433 (1991).
13. M. R. Jenkins *et al.*, *J. Immunol.* **181**, 3818 (2008).
14. M. A. Williams, A. J. Tyznik, M. J. Bevan, *Nature* **441**, 890 (2006).
15. L. E. Harrington, K. M. Janowski, J. R. Oliver, A. J. Zajac, C. T. Weaver, *Nature* **452**, 356 (2008).
16. The authors thank D. Winton for ROSA26EYFP mice, B. Crombrugghe for the CreER^{T2} construct, G. Eberl for the recombineering shuttle vector, and P. Digard and E. Hutchinson for help with viruses. This work was funded by the Wellcome Trust.

Supporting Online Material
www.sciencemag.org/cgi/content/full/323/5913/505/DC1
Materials and Methods
Figs. S1 to S3
Table S1
References

6 October 2008; accepted 1 December 2008
10.1126/science.1166831

Electron Cryomicroscopy of *E. coli* Reveals Filament Bundles Involved in Plasmid DNA Segregation

Jeanne Salje,*† Benoît Zuber, Jan Löwe

Bipolar elongation of filaments of the bacterial actin homolog ParM drives movement of newly replicated plasmid DNA to opposite poles of a bacterial cell. We used a combination of vitreous sectioning and electron cryotomography to study this DNA partitioning system directly in native, frozen cells. The diffraction patterns from overexpressed ParM bundles in electron cryotomographic reconstructions were used to unambiguously identify ParM filaments in *Escherichia coli* cells. Using a low–copy number plasmid encoding components required for partitioning, we observed small bundles of three to five intracellular ParM filaments that were situated close to the edge of the nucleoid. We propose that this may indicate the capture of plasmid DNA within the periphery of this loosely defined, chromosome-containing region.

One of the simplest known mechanisms by which newly replicated DNA molecules are moved apart is encoded by the bacterial low–copy number plasmid R1. This type II plasmid partitioning system includes three components that are both necessary and sufficient to confer genetic stability and are encoded in a tight gene cluster (*1*). ParM is an actin-like adenosine triphosphatase (ATPase) protein that forms double-helical filaments (*2*–*4*) and exhibits dynamic instability from both ends in the presence of ATP (*5*). Upon addition of both the small DNA-binding protein ParR and the centromere-like DNA region, *parC*, a ParR*C* protein-DNA complex caps and stabilizes both ends of the ParM filament (*6*–*8*). Thus stabilized, the ParM filament elongates at both ends and drives the plasmid-attached ParR*C* complexes to opposite poles of the bacterial cell. This system has been extensively studied both in cells using light microscopy (*9*–*11*) and in vitro (*5*, *6*), and here we turn to a direct characterization of ParMR*C*-driven DNA segregation in situ using vitreous sectioning (*12*) and electron cryotomography.

First, we set about characterizing ParM filaments directly in *E*scherichia *coli* cells that had been immobilized in a near-to-native vitreous state by high-pressure freezing (*13*). ParM was overexpressed to very high concentrations in the absence of ParR or *parC*. ParM filaments form spontaneously at these high concentrations. Images of cryosections revealed that these cells contained a large volume of tightly packed bundles of filaments (Fig. 1A and fig. S1A). This packing is probably due to the crowded environment of the cell. A small amount of crowding agent is sufficient to induce bundling of purified ParM filaments (Fig. 1, B and C) (*14*). Unlike actin, no additional proteins that induce bundling by cross-linking along the filaments of ParM are known or required.

To verify the identity of the bundles of filaments as ParM protein, we compared the diffraction patterns from electron cryomicrographs of in vitro bundles with those extracted from in situ electron cryotomography reconstructions. The resulting lateral diffraction spacing corresponds to packing of the roughly 80 Å thick filaments and was determined to be 83 Å in the tomogram slice (Fig. 1, D and E) and smeared between 63 and 83 Å for the in vitro bundles (Fig. 1, E and F). This smear relates to the fact that in vitro bundles were several filaments thick, producing additional, smaller interfilament repeats in the diffraction pattern. The longitudinal repeat of filamentous ParM was measured to be 53 Å in the in vitro bundles (Fig. 1E), agreeing with previous measurements on single filaments (*2*, *4*). We were able to measure the longitudinal repeat in tomographic slices, and this ranged from 41 to 53 Å, depending on the angle of rotation. The upper value confirmed the identity of these filaments. Bundles of filaments persisted in the presence of the MreB-depolymerizing drug A22 (fig. S1B), ruling out the possibility that these filaments were composed of the chromosomally encoded bacterial actin MreB.

As a comparison, we performed electron cryotomography on whole, intact plunge-frozen cells containing bundles of ParM (Fig. 1G). These cells expressed an ATPase-deficient mutant form of ParM [Asp^{170} → Ala^{170} (D170A)] (*11*), which is unable to depolymerize, leading to strings of cells with blocked septa. Even here the sample was too thick to achieve resolutions comparable to those obtained using thin cryosections, and the longitudinal repeat in the diffraction pattern could not be detected (compare Fig. 1, E and G).

Having identified ParM filaments directly in cryo-immobilized cells, we next turned to studying intracellular ParM filaments that are actively involved in segregating plasmid DNA. We used three different systems, each moving closer to the situation of the original R1 low-copy plasmid system (Fig. 2A). The first system was T7-driven ParM overexpression (see above). Next, we put three copies of the ParMR*C* cluster on a high–copy number plasmid (pBR322 replicon). Finally, a low–copy number R1-derived plasmid stabilized by a single copy of the ParMR*C* partitioning complex was used (pKG491) (*1*, *15*). A marked decrease in ParM levels was observed, moving from the overexpression system through the high–copy number plasmid to the low–copy number R1-derived plasmid (Fig. 2A). Cross sections through frozen cells overexpressing ParM protein clearly revealed tightly packed bundles of ParM (Fig. 2B, left, and fig. S1A). These images told us that ParM filaments would be best recognized in cross sections through the filaments (Fig. 2C). Cells carrying the ParMR*C*-containing high–copy number plasmid contained a combination of small bundles and single filaments within a single cell (Fig. 2B, middle, and fig. S2, A to C). Moving to even lower ParM concentrations using cells carrying the low–copy number R1 plasmid pKG491, we anticipated that observing filaments would be an extremely rare event. Previous studies have shown that pole-to-pole filaments of ParM can be observed in only ~40% of cells, with the others localizing in discrete clusters or diffuse throughout the cell (*11*). Furthermore, our ParM overexpression experiments told us that filaments could only be confidently recognized in those sections where the filament is exactly perpendicular to the imaging plane. Given that cells are frozen and sectioned in a semi-random orientation, we therefore imaged 300 to 400 cells.

Medical Research Council (MRC) Laboratory of Molecular Biology, Hills Road, Cambridge CB2 0QH, UK.

*To whom correspondence should be addressed. E-mail: jsalje@mrc-lmb.cam.ac.uk

†Present address: Kyoto University, Department of Biophysics, Faculty of Science, Oiwake Kitashirakawa, Sakyo-Ku, Kyoto 606-8502, Japan.